Science and Technology Indonesia
e-ISSN:2580-4391 *p*-ISSN:2580-4405
Vol. 9, No. 2, April 2024

Research Paper

Study on Crystal Structure, Surface Area, and Energy Gap Behaviors of Nanotitania Polymorphs Prepared Using Monoethanolamine

Posman Manurung[1]*, Renita Maharani[1], Dita Rahmayanti[1], Yanti Yulianti[1], Junaidi[1], Roniyus Marjunus[1]

[1]*Department of Physics, University of Lampung, Bandar Lampung, 35145, Indonesia*
***Corresponding author**: reip65@yahoo.com

Abstract
Polymorphous nanotitania samples were prepared from titanium butoxide (TTB) as a precursor using sol-gel processing in ethanol as a solvent, without and with monoethanolamine (MEA). The experiments used 5.25 mL TTB and MEA with varied volumes of 0.5, 1.0, 1.5, and 2.0 mL. The sample without MEA was specified as sample A, and the samples produced using MEA were specified as samples B, C, D, and E, respectively. All samples were calcined at 500 °C for 4 h and then collected data by X-ray Diffraction (XRD), the Brunauer-Emmett-Teller (BET) method used to analyze Surface Area Analyzer (SAA), Transmission Electron Microscopy (TEM), Raman Spectroscopy, and UV-Visible Diffuse Reflectance Spectroscopy (UV-Vis DRS). The results of XRD characterization indicate that samples A and B form anatase phase, while samples C and D are composed of anatase, brookite, and rutile phases, and sample E is consisted of anatase and brookite phases with weight percentages of (94.53 ± 1.72) % and (5.47 ± 0.36) %, respectively. The presence of the three phases of titania is also confirmed by Raman spectroscopy analysis, which showed anatase peaks at 146, 197, 398, and 513 cm^{-1}, brookite peaks at 245 and 402 cm^{-1}, and rutile peaks at 319, 436, and 612 cm^{-1}. According to XRD, the samples have the particle size in the range of 14-19 nm. A representative sample (sample C) was also characterized using TEM, revealing a particle size of 16.0 ± 0.3 nm. This representative sample revealed the largest surface area of 172.2 m^2/g, as seen by BET, and the lowest energy gap of 3.03 eV.

Keywords
Anatase, Brookite, Rutile, MEA, Nanotitania, Energy Gap

Received: 19 November 2023, Accepted: 27 February 2024
https://doi.org/10.26554/sti.2024.9.2.345-353

1. INTRODUCTION

Nano-scale titanium dioxide (TiO_2) has attracted the interest of the industry and the research society over the past decade since this material has been widely used for various purposes, including hydrogen production, self-cleaning surfaces, photocatalysis, and gas sensors (Ge et al., 2017; Fretwell and Douglas, 2001; Manurung et al., 2015; Yu et al., 2020; Maziarz, 2019).

Structurally, TiO_2 has polymorphic forms such as brookite, anatase, rutile (Zhang and Banfield, 1998). Structurally, crystal of anatase and rutile is tetragonal, and brookite is orthorhombic. The anatase and brookite are metastable phases that quickly change to the rutile phase when heated (Myint et al., 2017).

Nanotitania can be synthesized by physical and chemical methods, each with advantages and disadvantages. Physical processes can produce large quantities of material, but the particle size is more significant than nanometer scales. Chemical methods, on the other hand, are adequate for the production of material with particle size on the nanometer scale but limited to relatively small quantities (Park et al., 2007). Hitherto, nano TiO_2 has been synthesized by various methods such as hydrothermal, solvothermal, direct oxidation, chemical vapor deposition, electrodeposition, and sol-gel (Byranvand et al., 2013). The sol-gel method is widely applied for the production of nanomaterial since this method offers advantages such as the possibility of obtaining homogeneous hybrid materials at low temperatures, low cost, and easy processing (Chaure et al., 2005). Using the sol-gel method, nano TiO_2 has been synthesized from the hydrolysis of titanium precursors. Símonarson et al. (2019) recently synthesized nanotitania polymorphs from titanium n-butoxide at low temperature (40 °C) in an acidic HCl environment with ethanol as a solvent. However, the XRD data indicated that the crystallinity of the sample was relatively low, and the intensity of the diffraction peak of the brookite was fragile. In addition, the preparation process requires a relatively long time, ranging from three to 56 days. Galkina et al. (2011) used the sol-gel method to synthesize nanotitania from titanium isopropoxide using polyethylenimine and pluronic P-123 surfactants. The experimental results indicate

that polyethylenimine led to the production of anatase and rutile phases, while the use of pluronic led to the formation of anatase, rutile, and brookite in minimal amounts.

A few researchers focused on using two or three surfactants to prepare nanotitania polymorphs. There have been limited studies concerned with using a single surfactant. Therefore, this research intends to synthesize nanotitania polymorphs using a single surfactant. Using two anatase-brookite polymorphs, directly mixing the powders of each phase will produce an interface, which, in turn, will influence the photocurrent properties of the material (Presti et al., 2021). The method proposed in this paper is expected to produce something other than an interface. This can be assumed as other novelty of this work. Other researchers also synthesized nanotitania using the surfactant of triethanolamine at heating of 500 °C for 4 h and only obtained anatase and rutile phases (Shirzad Taghanaki et al., 2021). González Anota et al. (2023) prepared nanotitania using cinnamon extract and $TiCl_4$ with a green synthesis method at 450 °C, producing anatase with a small amount of rutile. From this fact, the novelty of this research is how to synthesize the three polymorphs of nanotitania with only a single surfactant.

This research aims to prepare the polymorphs of nanotitania at a time. In order to increase the quantity of brookite, varied volumes of 0.5, 1, 1.5, and 2 mL were used to synthesize nanotitania from titanium butoxide, employing a single nonionic surfactant, monoethanolamine (MEA). This research was conducted to see the influence of MEA in terms of phase composition, surface area, and energy gap of the nanotitania produced. The experiments were conducted in ethanol as a solvent, and the products obtained were then characterized to obtain information regarding crystal structure. Characterizations using Raman spectroscopy as complementary to XDR, BET, TEM. UV-Visible Diffuse Reflectance Spectroscopy (UV-Vis DRS) were also conducted in determining of surface area and energy gap.

2. EXPERIMENTAL SECTION

2.1 Materials

Titanium butoxide ($C_{16}H_{36}O_4Ti$) was purchased from Sigma Aldrich, ethanol (C_2H_5OH), monoethanolamine (C_2H_7NO), and HCl 37% were found from Merck. There is no more treatment to all chemicals because they were considered fairly pure.

2.2 Instrumentations

XRD data are obtained from 10-90° in step of 0.02° by using XRD XPERT PRO PANanalytical (The Netherlands) using CuKα radiation (λ = 1.54060 Å) at 40 kV and 30 mA. XRD characterization uses powder techniques. TEM used is JEOUL JEM-1400 (Japan) aimed to find the particle size. The Scherrer equation was used to count particle size of samples:

$$D = \frac{0.9\lambda}{B\,cos\theta} \quad (1)$$

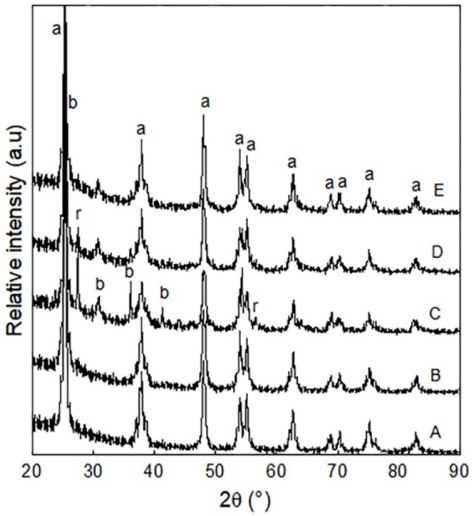

Figure 1. Diffractograms of the Samples Synthesized without MEA (A) and with MEA (B, C, D, and E). Captions: a for Anatase, b for Brookite, and r for Rutile.

with λ = the wavelength of X-ray, B = the width of peak at half maximum, and θ = scattering angle.

Surface area of sample was characterized by N_2 adsorption using Quantachrome TouchWin v1.2 (USA) at temperature of 77 K. The experiment was conducted at an ambient temperature of 29.16 °C using a 9 mm rod-type cell and vacuum degassing mode. In this case, the molecular weight of nitrogen is 28.013 g/mol, and the cross-section area is 16.2 $Å^2$/mol. BET (S) is calculated based on the Equation 2.

$$S = V_m.N.A/M \quad (2)$$

where V^m = slope of the curve, N = Avogadros's number = 6.02×10^{23}/mol, A = cross section and M = molecular weight of nitrogen.

Energy gap of samples was calculated based on UV-Vis DRS data that collected by instrument of Cary 100 (Australia). As a complement to XRD data in obtaining the presence of the nanotitania phase, Raman spectroscopy was also used by using the LabRAM HR Evolution Raman Microscope (Japan), which has dual laser multidetector in the wavelengths of 532-758 nm.

2.3 Methods

The precursor solution was prepared by adding titanium butoxide (TTB) of 5.25 mL to ethanol of 60 mL. Both chemicals were stirred for 30 minutes in a beaker glass. While stirring, MEA with volume in the range of 0 to 2 mL was added dropwise. The aim is to achieve homogeneous solutions. Finally, 2.45 mL of HCl was added, and the solution was continuously stirred overnight. Adding chloride acid is intended to improve the three polymorphs' content. Table 1 showed the compositions of all samples.

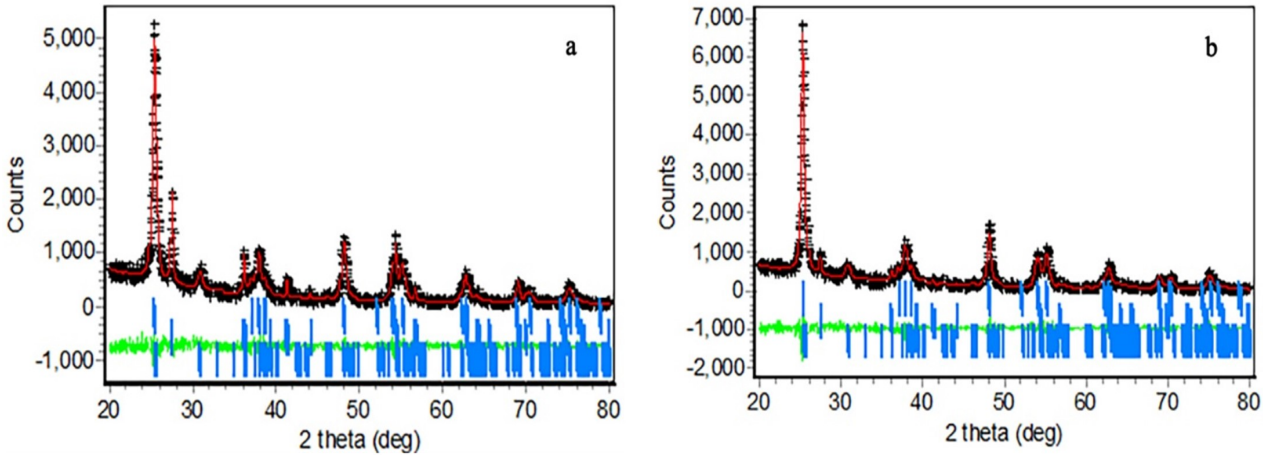

Figure 2. XRD Difference Plot for Nanotitania Polymorph (a) Sample C and (b) D. The Black and Red Colors Represent the Data and Model Used. Blue Bars Are Bragg Angle Positions for Each Phase (from Top to Bottom: Anatase, Rutile, and Brookite).

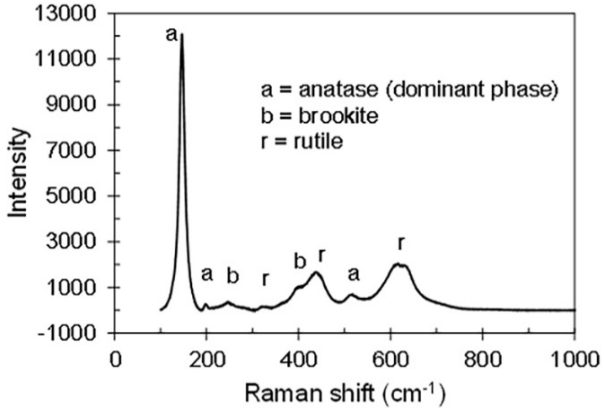

Figure 3. Raman Spectroscopy of Sample C with MEA 1 mL

Table 1. Compositions of Reaction Mixtures Used in the Study

Sample	TTB (mL)	Ethanol (mL)	HCl 37% (mL)	MEA (mL)
A	5.25	60	2.45	0.0
B	5.25	60	2.45	0.5
C	5.25	60	2.45	1.0
D	5.25	60	2.45	1.5
E	5.25	60	2.45	2.0

After the completion of the preparation process, the samples were oven-dried at 100 °C for 12 h and continued at 200 °C for 24 h. The samples were then calcined at 500 °C for 4 h and finally grounded with mortar and agate pestle to obtain characterization powder.

3. RESULTS AND DISCUSSION

3.1 XRD Studies

3.1.1 Qualitative Analysis

In this study, five samples prepared were characterized using the XRD technique, producing diffractograms as presented in Figure 1. A qualitative analysis will be carried out regarding the phases present in each sample, and a quantitative analysis will determine the percentage by weight of each step.

The XRD diffractograms depicted in Figure 1 indicate that the samples are consisted of brookite phase (JCPDS No. 29-1360), anatase (JCPDS No. 21-1272), and rutile (JCPDS No. 21-1276) (Swanson et al., 1969; Swanson et al., 1964). The position of the diffraction peaks in each sample is relatively the same, indicating that the distance between the crystal planes is relatively the same. The highest peak of anatase is located in the 2θ position of around 25.30° to 25.34°, which agrees with the findings of other workers (Manurung et al., 2020). The highest peak of rutile is in the position between (27.42 - 27.44)°, and the highest peak of brookite is in the position between (25.34-30.82)°, both are also in agreement with those reported in several previous studies (Galkina et al., 2011; Abdel Azim et al., 2014; Hu et al., 2003).

As shown in Figure 1, using 0.5 mL of MEA (sample B) only resulted in the anatase phase. Interestingly, an adequate quantity of brookite and rutile phases in samples C and D, in addition to the anatase phase, was observed. In several previous studies, it was reported that the rutile phase appeared at temperatures above 500 °C, and brookite appeared below 500 °C (Bakardjieva et al., 2006; Dastan et al., 2017; Mutuma et al., 2015). However, in this study, especially in samples C and D, rutile and brookite phases appeared at a temperature of 500 °C. These results indicate that using 1.0 and 1.5 mL MEA is sufficient to produce polymorphic nanotitania. The use of nonionic MEA surfactants in the synthesis of TiO_2 with more than one phase has also been found by others (Galkina

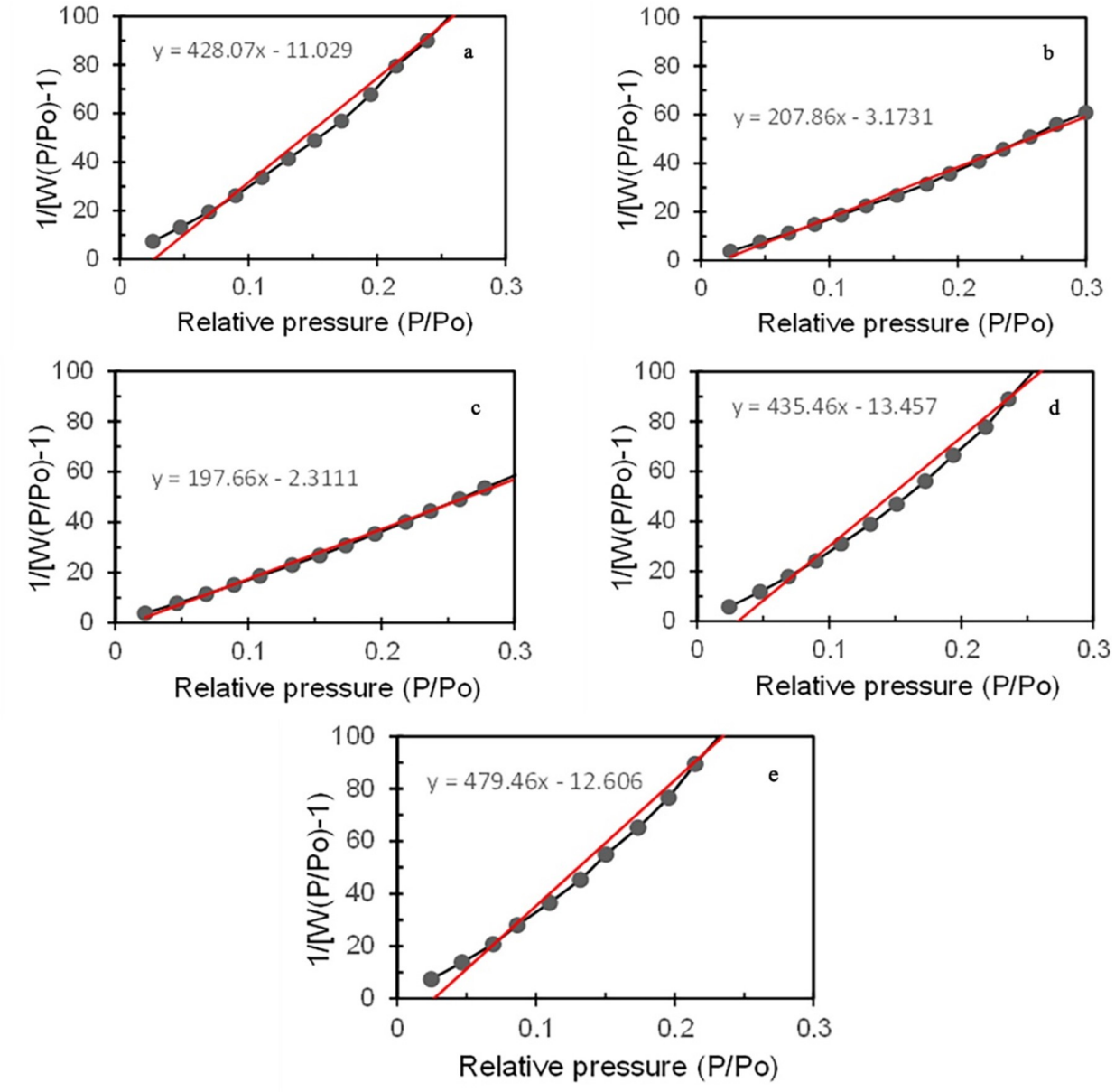

Figure 4. BET Profile Samples (a) A = 83.5 m^2/g, (b) B = 170.1 m^2/g, (c) C = 172.2 m^2/g, (d) D = 82.5 m^2/g, and (e) E = 74.5 m^2/g

et al., 2011; Abdel Azim et al., 2014; Burczyk et al., 2001).

The mixture of surfactant and HCl causes the sample to undergo partial hydrolysis. Partial hydrolysis occurs if the weakly alkaline solution is added to the strong acid. The rutile phase can appear if the sample has a low degree of hydrolysis during the synthesis process, causing a nucleation process in which rutile is formed in the anatase phase (Bidaye and Fernandes, 2019; Sahni et al., 2007). Another factor reported to promote the formation of brookite and rutile phases below 500 °C is pH (Hu et al., 2003). In research conducted by Galkina et al. (2011), the samples added with pluronic surfactants at low pH values between 1-2 were found to result in the formation of brookite and rutile phases. According to Hu et al. (2003), the synthesis of TiO_2 with a low pH can produce brookite and rutile phases, where the brookite phase appears at a pH of 2 and a heating temperature of 500 °C. The brookite phase does not appear at greater pH and higher calcination temperature. In this study, adding MEA resulted in a pH of 2.

Furthermore, the addition of MEA in considerable amounts, as the aim of this research, can influence the pH of the solution, while surfactant mixed with HCl might cause partial hydrolysis to form anatase and rutile. Usually, the pH of MEA and HCl is 8 and 2, respectively. This unique combination promoted the crystallization of brookite beside anatase and rutile. That

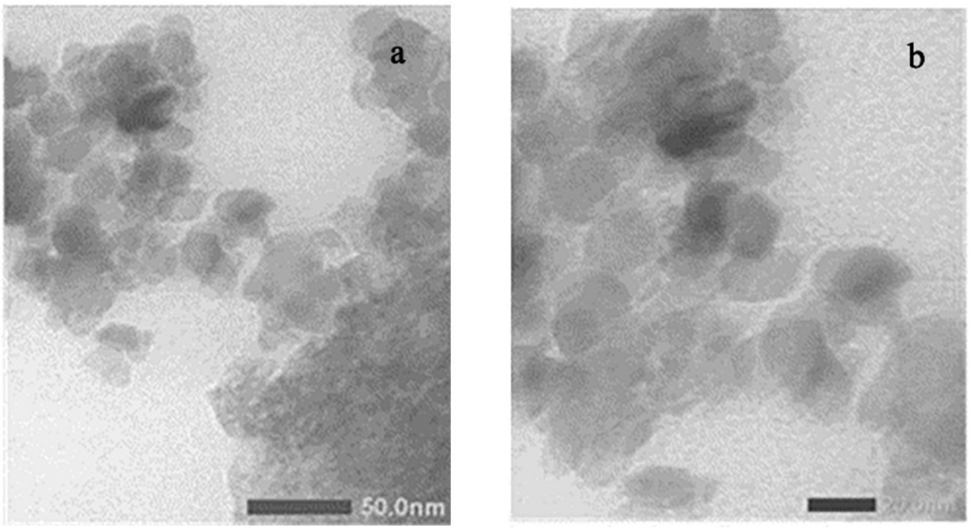

Figure 5. TEM of Sample C with MEA 1 mL (a) Bar Scale of 50 nm and (b) 20 nm

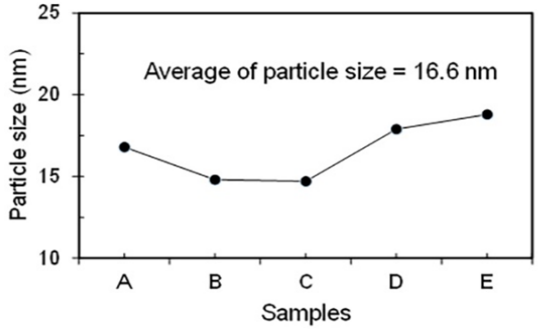

Figure 6. Particle Size According to XRD Data

is the reason that the presence of MEA at 1.0 and 1.5 mL can produce nanotitania polymorphs.

3.1.2 Quantitative Analysis

Rietveld method was used to determine the composition of each phase. Rietica software was used to refine XRD data (Hunter, 1997). The refinement model used for the anatase phase was Djerdj and Tonejc (2006), Howard et al. (1991) for rutile, and Meagher and Lager (1979) for brookite. The pseudo-Voigt function was used to model the shape of diffraction peaks. The refinement results of samples C and D are shown in Figure 2, while other samples are not shown in this study.

Figure 2 shows the refinement results are successfully, indicated by the decreasing of the R factors (Rp, Rwp, Rexp, and RB) during the calculation process. The calculation of the weight percentage of each phase in samples C, D, and E are compiled in Table 2. Table 2 shows the abundance of brookite, anatase and rutile in the sample. The relative percentage of the brookite phase observed in this study is enough higher than that

Table 2. Relative Phase Abundance for Samples in Weight Percentage (% wt)

Sample	Anatase (% wt)	Rutile (% wt)	Brookite (% wt)
C	65.77 ± 2.12	16.91 ± 0.98	17.32 ± 0.87
D	83.91 ± 1.22	6.04 ± 0.37	10.05 ± 0.72
E	94.53 ± 1.72	-	5.47 ± 0.36

worked by others (Abdel Azim et al., 2014). The use of 1.0, 1.5, and 2.0 mL MEA resulted in the formation of brookite with the other two phases, with the optimum weight percentage of brookite in sample C. The weight percentage of anatase increases with the addition of MEA, but on the other hand, decreases the rutile and brookite phases. It could be because the rutile and brookite phases changed to anatase with more MEA. In other words, adding MEA surfactant will increase the stability of the anatase to produce smaller brookite and rutile phases because the stability of the anatase will increase with increasing surfactant used. The presence of the brookite is more significant than that in the sample produced with the use of pluronic surfactant P-123 and polyethyleneimine (Galkina et al., 2011), suggesting that different surfactants may impart different effects. Adding 1 mL MEA to the calcined nanotitania resulted in the simultaneous presence of brookite, anatase and rutile phases.

3.2 Raman Spectroscopy Analysis as Complementary to XRD

Raman spectroscopic analysis was carried out to complement XRD data since Raman spectroscopy is helpful to detect the amorphous and crystalline parts of a material, while XRD only detects the crystalline part. The data obtained from Raman spectroscopy is a plot of the peak intensity and Raman shift. Qualitative analysis was done by matching the experimental

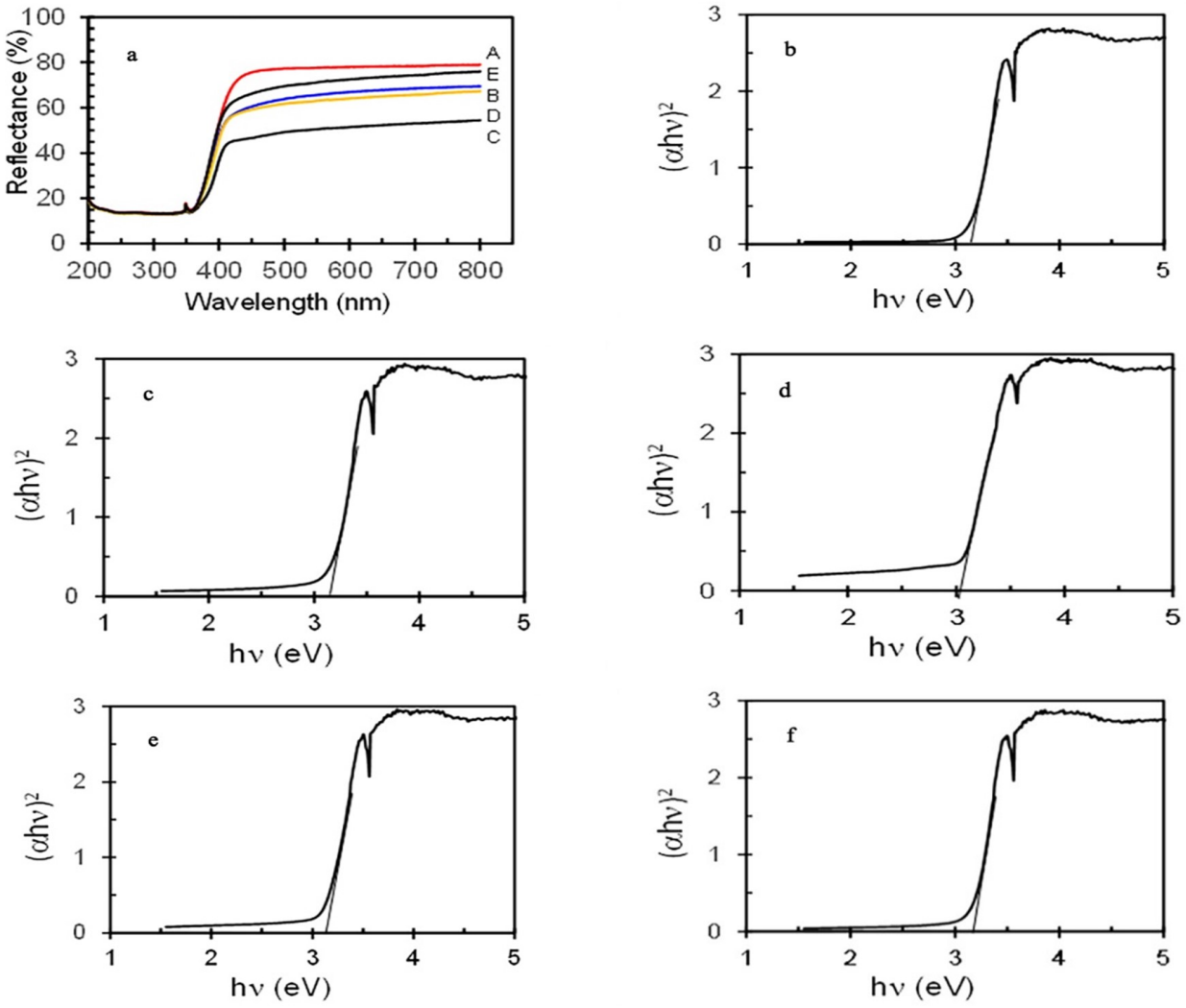

Figure 7. (a) UV-DRS Spectrum of All Samples. Tauc Plot for Calculating Eg of Samples A = 3.18 eV (b), B = 3.20 eV (c), C = 3.03 eV (d), D = 3.15 eV (e), and E = 3.20 eV (f)

Raman shift's value with the results of previous studies.

The anatase phase with 12 atoms per unit cell has six vibrational modes, brookite with 8 atoms per unit cell has 36 vibrational modes, and rutile with 6 atoms has 15 vibrational modes (Rezaee et al., 2011). Figure 3 shows the Raman spectroscopy of sample C (MEA added 1 mL).

The peaks of the sample in the spectrum are not the same as the reference, most likely because the starting materials used are different from this study. After matching the data with previous studies, the peak characteristic of anatase was shown at the Raman shift values of 146, 197, and 513 cm^{-1} (Yazid et al., 2019; Zhu et al., 2005). The brookite phase is represented by the peaks at 245 and 402 cm^{-1}, while rutile is represented by the peaks located at 319, 436, and 613 cm^{-1} (Rezaee et al., 2011; Golubović et al., 2009; Zhang et al., 2011). This study proves significantly the presence of nanotitania polymorph in sample C with MEA 1 mL.

3.3 Surface Area Analysis

The BET method was used to acquire the specific surface area and calculated using a nitrogen adsorption-desorption process at 77 K using SAA Quantachrome NOVA 1000e version 11.0. Figure 4 shows the BET profile of the samples investigated. Equation 2 was used to calculate specific surface area. The smallest surface area (72.1 m^2/g) was found in sample E, while the largest (172.2 m^2/g) was obtained in sample C. The general trend observed is increased surface area to a maximum at the addition of 1 mL MEA and then decreased again as the volume of MEA increased.

The maximum surface area of the sample synthesized is more significant than that of the same samples using $TiOSO_4$ as a source of titania and the use of sulfuric acid, acetic acid, and glycolic acid (Yu et al., 2020) instead of TTB used in this study. The maximum brookite and rutile phases in sample C most likely contribute to this particular sample's higher surface

than the other samples.

3.4 Particle Size Analysis

Figure 5 shows the results of TEM analysis on sample C (addition of MEA 1 mL) with a bar scale of 50 and 20 nm. Particle size calculations are taken based on both scales for more accurate results. The two images show particle sizes of (15.0 ± 0.2) nm and (17.0 ± 0.4) nm, respectively. Thus, the average particle size is (16.0 ± 0.3) nm, which belongs to the classification of nanoparticles. From the two TEM images, it appears that there is adhesion between the particles so that the particles do not experience adhesion, and the shape of the particles, in general, is spherical (Huseynov et al., 2016).

Compared to TEM results, the particle size was also calculated based on the XRD data (Figure 1). The particle size calculation is based on the Scherrer formula (Equation 1), and overall results are presented in Figure 6. It can be seen from Figure 6 that the particle size is in the range of 14-19 nm, with sample C having the smallest size. This size is consistent with the size according to the TEM measurement (16.0 ± 0.3) nm. TEM results imply a relationship between particle size and sample surface area, in which the smaller the particle size, the larger the sample surface area. These results agree with the result reported by other (Yu et al., 2020).

3.5 Energy Gap Analysis

Figure 7 presents the UV-DRS spectrum of all samples and the Tauc plot for calculating the energy gap (Eg). The energy gap is calculated using the Kubelka-Munk method and plotted with Tauc (Makuła et al., 2018) based on the UV-Vis DRS data produced by the Cary 100 spectrometer. Eg is tangent line to curve until it intersects the x-axis or energy in *hv* unit.

It can be seen that the Eg ranges from 3.00-3.20 eV, in agreement with the energy gap of the TiO_2 standard, which is 3.20 eV (Dette et al., 2014). The exciting thing from this study is that the lowest Eg was obtained in sample C or the addition of 1 mL of MEA. This result corresponds to the smallest sample particle size, where brookite, anatase, and rutile Eg are 3.20, 3.50, and 3.31 eV, respectively. The value of nano-sized Eg titania will be lower than that of micro-sized titania (Nagaveni et al., 2004).

The Eg value in this study is slightly lower than the standard anatase of 3.20 eV even though it has been mixed with brookite and rutile phases. So, the presence of brookite and rutile phases in titania polymorphs can reduce the value of Eg. In addition, the calcination temperature can also affect the value of Eg titania as reported by Xia et al. (2013), where Eg titania at temperatures of 90, 200, 400, and 550 °C are 3.67; 3.59; 3.40 and 3.35 eV, respectively. These results demonstrate that MEA can affect the Eg value of the nanotitania synthesized.

4. CONCLUSIONS

Based on the results of experiments and optical Nanotitania polymorphs were successfully synthesized from titanium butoxide as a precursor using a single surfactant MEA. Samples without and with MEA of 0.5 mL are pure crystalline anatase, while samples with MEA of 1.0 and 1.5 mL comprise the polymorphs of brookite, anatase, and rutile. The sample with MEA 2.0 mL comprises the two polymorphs of anatase and brookite. The addition of MEA affected particles size, in which the addition of 1.0 mL of MEA produced the titania with a particle size of 16 ± 1 nm. Adding 1 mL of MEA resulted in the largest specific surface area of 172.2 m^2/g and decreased with increasing volumes of MEA used. Raman spectroscopy convincingly proves the presence of the three polymorphs. The smallest energy gap (3.03 eV) was obtained in the sample with 1 mL MEA. This study successfully synthesized high crystalline polymorphic nanotitania with appreciable quantities of all three phases. Another impressive finding of this study is the successful preparation of polymorphic nanotitania with a single surfactant, while other researchers reported using two types of surfactants for the same purpose.

5. ACKNOWLEDGMENT

The author would like to thank Dikti for funding this research through the DIKTI Postgraduate Research Grant scheme.

REFERENCES

Abdel Azim, S., A. Aboul Gheit, S. Ahmed, D. El Desouki, and M. Abdel Mottaleb (2014). Preparation and Application of Mesoporous Nanotitania Photocatalysts Using Different Templates and Ph Media. *International Journal of Photoenergy*, **2014**; 1–11

Bakardjieva, S., V. Stengl, L. Szatmary, J. Subrt, J. Lukac, N. Murafa, D. Niznansky, K. Cizek, J. Jirkovsky, and N. Petrova (2006). Transformation of Brookite-Type TiO_2 Nanocrystals to Rutile: Correlation between Microstructure and Photoactivity. *Journal of Materials Chemistry*, **16**(18); 1709–1716

Bidaye, P. P. and J. B. Fernandes (2019). A Rapid and Facile Synthesis Method for Nanosize Rutile Phase TiO_2 with High Photocatalytic Activity. *Green and Sustainable Chemistry*, **9**(2); 27–37

Burczyk, B., K. A. Wilk, A. Sokołowski, and L. Syper (2001). Synthesis and Surface Properties of *N*-Alkyl-*N*-Methylgluconamides and *N*-Alkyl-*N*-Methyllactobionamides. *Journal of Colloid and Interface Science*, **240**(2); 552–558

Byranvand, M. M., A. Nemati Kharat, L. Fatholahi, and Z. Malekshahi Beiranvand (2013). A Review on Synthesis of Nano-TiO_2 Via Different Methods. *Journal of Nanostructures*, **3**(1); 1–9

Chaure, N., A. Ray, and R. Capan (2005). Sol-Gel Derived Nanocrystalline Titania Thin Films on Silicon. *Semiconductor Science and Technology*, **20**(8); 788

Dastan, D., N. Chaure, and M. Kartha (2017). Surfactants Assisted Solvothermal Derived Titania Nanoparticles: Synthesis and Simulation. *Journal of Materials Science: Materials in Electronics*, **28**(11); 7784–7796

Dette, C., M. A. Pérez Osorio, C. S. Kley, P. Punke, C. E. Patrick, P. Jacobson, F. Giustino, S. J. Jung, and K. Kern (2014). TiO_2 Anatase with a Bandgap in the Visible Region. *Nano Letters*, **14**(11); 6533–6538

Djerdj, I. and A. Tonejc (2006). Structural Investigations of Nanocrystalline TiO_2 Samples. *Journal of Alloys and Compounds*, **413**(1-2); 159–174

Fretwell, R. and P. Douglas (2001). An Active, Robust and Transparent Nanocrystalline Anatase TiO_2 Thin Film-Preparation, Characterisation and the Kinetics of Photodegradation of Model Pollutants. *Journal of Photochemistry and Photobiology A: Chemistry*, **143**(2-3); 229–240

Galkina, O., V. Vinogradov, A. Agafonov, and A. Vinogradov (2011). Surfactant-Assisted Sol-Gel Synthesis of TiO_2 with Uniform Particle Size Distribution. *International Journal of Inorganic Chemistry*, **2011**; 1–8

Ge, M., J. Cai, J. Iocozzia, C. Cao, J. Huang, X. Zhang, J. Shen, S. Wang, S. Zhang, and K. Q. Zhang (2017). A Review of TiO_2 Nanostructured Catalysts for Sustainable H_2 Generation. *International Journal of Hydrogen Energy*, **42**(12); 8418–8449

Golubović, A., M. Šćepanović, A. Kremenović, S. Aškrabić, V. Berec, Z. Dohčević Mitrović, and Z. Popović (2009). Raman Study of the Variation in Anatase Structure of TiO_2 Nanopowders Due to the Changes of Sol-Gel Synthesis Conditions. *Journal of Sol-Gel Science and Technology*, **49**; 311–319

González Anota, D. E., S. P. Paredes Carrera, R. M. Pérez Gutierrez, B. Arciniega-Caballero, R. Borja Urby, J. C. Sánchez-Ochoa, and E. Rojas García (2023). Green Synthesis by Microwave Irradiation of TiO_2 Using Cinnamomum Verum and the Application in Photocatalysis. *Journal of Chemistry*, **2023**; 1–17

Howard, C., T. Sabine, and F. Dickson (1991). Structural and Thermal Parameters for Rutile and Anatase. *Acta Crystallographica Section B: Structural Science*, **47**(4); 462–468

Hu, Y., H. L. Tsai, and C. L. Huang (2003). Effect of Brookite Phase on the Anatase-Rutile Transition in Titania Nanoparticles. *Journal of the European Ceramic Society*, **23**(5); 691–696

Hunter, B. (1997). Rietica for Windows Version 4.0. *IUCR Powder Diffraction*, **22**(1)

Huseynov, E., A. Garibov, and R. Mehdiyeva (2016). TEM and SEM Study of Nano SiO_2 Particles Exposed to Influence of Neutron Flux. *Journal of Materials Research and Technology*, **5**(3); 213–218

Makuła, P., M. Pacia, and W. Macyk (2018). How to Correctly Determine the Band Gap Energy of Modified Semiconductor Photocatalysts Based on UV-Vis Spectra. *The Journal of Physical Chemistry Letters*, **9**(23); 6814–6817

Manurung, P., R. Situmeang, E. Ginting, and I. Pardede (2015). Synthesis and Characterization of Titania-Rice Husk Silica Composites As Photocatalyst. *Indonesian Journal of Chemistry*, **15**(1); 36–42

Manurung, P., R. Situmeang, P. Sinuhaji, and S. Sembiring (2020). Effect of Sulfur Doped Nanotitania for Degradation of Remazol Yellow and Phenol. *Asian Journal of Chemistry*, **32**(12); 3019–3023

Maziarz, W. (2019). TiO_2/SnO_2 and TiO_2/CuO Thin Film Nano-Heterostructures As Gas Sensors. *Applied Surface Science*, **480**; 361–370

Meagher, E. and G. A. Lager (1979). Polyhedral Thermal Expansion in the TiO_2 Polymorphs; Refinement of the Crystal Structures of Rutile and Brookite at High Temperature. *The Canadian Mineralogist*, **17**(1); 77–85

Mutuma, B. K., G. N. Shao, W. D. Kim, and H. T. Kim (2015). Sol-Gel Synthesis of Mesoporous Anatase-Brookite and Anatase-Brookite-Rutile TiO_2 Nanoparticles and Their Photocatalytic Properties. *Journal of Colloid and Interface Science*, **442**; 1–7

Myint, Y. W., T. T. Moe, W. Y. Linn, A. Chang, and P. P. Win (2017). The Effect of Heat Treatment on Phase Transformation and Morphology of Nano-Crystalline Titanium Dioxide (TiO_2). *International Journal of Scientific & Technology Research*, **6**(6); 293–299

Nagaveni, K., M. Hegde, N. Ravishankar, G. Subbanna, and G. Madras (2004). Synthesis and Structure of Nanocrystalline TiO_2 with Lower Band Gap Showing High Photocatalytic Activity. *Langmuir*, **20**(7); 2900–2907

Park, J., J. Joo, S. G. Kwon, Y. Jang, and T. Hyeon (2007). Synthesis of Monodisperse Spherical Nanocrystals. *Angewandte Chemie International Edition*, **46**(25); 4630–4660

Presti, L. L., V. Pifferi, G. Di Liberto, G. Cappelletti, L. Falciola, G. Cerrato, and M. Ceotto (2021). Direct Measurement and Modeling of Spontaneous Charge Migration across Anatase-Brookite Nanoheterojunctions. *Journal of Materials Chemistry A*, **9**(12); 7782–7790

Rezaee, M., S. M. M. Khoie, and K. H. Liu (2011). The Role of Brookite in Mechanical Activation of Anatase-to-Rutile Transformation of Nanocrystalline TiO_2: An Xrd and Raman Spectroscopy Investigation. *CrystEngComm*, **13**(16); 5055–5061

Sahni, S., S. B. Reddy, and B. Murty (2007). Influence of Process Parameters on the Synthesis of Nano-Titania by Sol-Gel Route. *Materials Science and Engineering: A*, **452**; 758–762

Shirzad Taghanaki, N., N. Keramati, and M. Mehdipour Ghazi (2021). Photocatalytic Degradation of Ethylbenzene by Nano Photocatalyst in Aerogel form Based on Titania. *Iranian Journal of Chemistry and Chemical Engineering*, **40**(2); 525–537

Símonarson, G., S. Sommer, A. Lotsari, B. Elgh, B. B. Iversen, and A. E. Palmqvist (2019). Evolution of the Polymorph Selectivity of Titania Formation under Acidic and Low-Temperature Conditions. *ACS omega*, **4**(3); 5750–5757

Swanson, H. E., H. F. McMurdie, M. C. Morris, and E. H. Evans (1969). *Standard X-ray Diffraction Powder Patterns*, volume 25. United States. Government Printing Office

Swanson, H. E., M. C. Morris, E. H. Evans, and L. Ulmer (1964). *Standard X-ray Diffraction Powder Patterns*, volume 25. United States. Government Printing Office

Xia, T., J. W. Otto, T. Dutta, J. Murowchick, A. N. Caruso, Z. Peng, and X. Chen (2013). Formation of TiO_2 Nanomaterials Via Titanium Ethylene Glycolide Decomposition. *Journal of Materials Research*, **28**(3); 326–332

Yazid, S. A., Z. M. Rosli, and J. M. Juoi (2019). Effect of Titanium (IV) Isopropoxide Molarity on the Crystallinity and Photocatalytic Activity of Titanium Dioxide Thin Film Deposited Via Green Sol-Gel Route. *Journal of Materials Research and Technology*, **8**(1); 1434–1439

Yu, J., A. L. Godiksen, A. Mamahkel, F. Søndergaard Pedersen, T. Rios Carvajal, M. Marks, N. Lock, S. B. Rasmussen, and B. B. Iversen (2020). Selective Catalytic Reduction of NO Using Phase-Pure Anatase, Rutile, and Brookite TiO_2 Nanocrystals. *Inorganic Chemistry*, **59**(20); 15324–15334

Zhang, H. and J. F. Banfield (1998). Thermodynamic Analysis of Phase Stability of Nanocrystalline Titania. *Journal of Materials Chemistry*, **8**(9); 2073–2076

Zhang, J., Y. Song, F. Lu, W. Fei, Y. Mengqiong, L. Genxiang, X. Qian, W. Xiang, and L. Can (2011). Photocatalytic Degradation of Rhodamine B on Anatase, Rutile, and Brookite TiO_2. *Chinese Journal of Catalysis*, **32**(6-8); 983–991

Zhu, K. R., M. S. Zhang, Q. Chen, and Z. Yin (2005). Size and Phonon-Confinement Effects on Low-Frequency Raman Mode of Anatase TiO_2 Nanocrystal. *Physics Letters A*, **340**(1-4); 220–227

